Heavy-ion transfer reactions studied at large internuclear distances with the PRISMA magnetic spectrometer

2013 J. Phys.: Conf. Ser. 420 012161

(http://iopscience.iop.org/1742-6596/420/1/012161)

Journal of Physics: Conference Series **420** (2013) 012161 doi:10.1088/1742-6596/420/1/012161

Heavy-ion transfer reactions studied at large internuclear distances with the PRISMA magnetic spectrometer

D. Montanari[2], L. Corradi[1], S. Szilner[5], G. Pollarolo[4], E. Fioretto[1], A.M. Stefanini[1], E. Farnea[2], C. Michelagnoli[2], G. Montagnoli[2], F. Scarlassara[2], C.A. Ur[2], S. Courtin[3], A. Goasduff[3], F. Haas[3], T. Mijatović[5], N. Soić[5] and J. Grebosz[6]

[1] Istituto Nazionale di Fisica Nucleare, Laboratori Nazionali di Legnaro, I-35020 Legnaro, Italy,
[2] Dipartimento di Fisica e Astronomia, Università di Padova, and Istituto Nazionale di Fisica Nucleare, I-35131, Padova, Italy,
[3] Institut Pluridisciplinaire Hubert Curien, CNRS-IN2P3, Université de Strasbourg, F-67037 Strasbourg, France,
[4] Dipartimento di Fisica Teorica, Università di Torino, and Istituto Nazionale di Fisica Nucleare, I-10125 Torino, Italy,
[5] Ruđer Bošković Institute, HR-10 002 Zagreb, Croatia,
[6] The Henryk Niewodniczanski Institute of Nuclear Physics, PL-31-342, Krakow, Poland.

E-mail: daniele.montanari@pd.infn.it

Abstract.
We performed a study of the behaviour of the main transfer channels in the ^{116}Sn+^{60}Ni system at different bombarding energies from above to well below the Coulomb barrier. The experiment has been done in inverse kinematics, detecting the lighter target-like ions with the magnetic spectrometer PRISMA at very forward angles. Good mass, nuclear charge and kinetic energy resolutions have been achieved. Sufficient statistics has been accumulated to extract angular distributions for different bombarding energies, requiring a study of the response function of the spectrometer. The comparison between the data and microscopic calculations for the present case and for the previously measured ^{96}Zr+^{40}Ca system, namely superfluid and near closed shells nuclei, should significantly improve our understanding of nucleon-nucleon correlation properties in multinucleon transfer processes.

1. Introduction

Transfer reactions, both with light and heavy ions, at energies close to the Coulomb barrier always played an important role for nuclear structure and reaction dynamic studies. While reactions with light ions have provided detailed information on the nuclear shell model and on particle-particle correlations, with heavy ions transfers of several nucleons become available in the reaction thus giving the possibility to study the role played by single and multi-nucleon transfer modes (see Ref. [1] and references therein for the last review on heavy ion transfer reactions). Most of the existing studies with heavy ions involve the measurements of inclusive cross-sections at and above the Coulomb barrier, where the theoretical interpretation becomes

much more difficult due to the presence of many competing processes. At energies below the Coulomb barrier nuclei are at large distances, so that they interact through the tail of their density distribution and are only slightly influenced by the nuclear potential. In this energy regime, reaction products are excited in a restricted energy region (few MeV) and therefore the complexity of coupled channel calculations is minimized, since one needs to take into account few populated excited states. Furthermore, at sub-barrier energies more quantitative information may be extracted on the correlations close to the ground states [2].

Traditionally, one extracts the transfer probability [3, 4] (P_{tr}, ratio of transfer to elastic cross sections) by measuring either excitation functions at fixed angles or angular distributions at fixed energies. The P_{tr} extracted with the two methods should be the same provided that ions interact at very large distances, where deep inelastic components drop off. Most of the data represented in the past by P_{tr} have been derived from angular distributions at energies above the Coulomb barrier, where processes other than the direct one may contribute to the cross section (see e.g. the discussion on slope anomalies in [5, 6]). Excitation functions at energies below the barrier have been performed in only a few cases [7, 8, 9, 10], due to stringent experimental difficulties and the limitation in efficiency of the available detection devices.

Since a few years, with the coming into operation of large acceptance magnetic spectrometers, we are in a condition to study multinucleon transfer reactions at energies far below the Coulomb barrier with a good mass identification, especially in inverse kinematic conditions where the lighter target-like recoils have high kinetic energy. The efficient use of the large solid angle spectrometer PRISMA to perform such studies has already been demonstrated in the study of the ^{96}Zr+^{40}Ca system [11]. Making use of inverse kinematics, excitation functions for the most intense transfer channels have been obtained by detecting target recoils and varying the bombarding energies in several steps from above to well below the barrier, corresponding to a broad range of distances of closest approach. The data have been compared with microscopic calculations performed within a semi-classical theory [12, 13], where the two particle transfer included the 0^+ states of both projectile and target. From the comparison, the role played by the $f_{7/2}$ and $p_{3/2}$ single particle states has been identified. While the first dominates the ground state wave function of ^{42}Ca the second dominates the wave function of the 0^+ state at 5.76 MeV. Such a state for the $+2n$ channel has a good match with the optimum Q-value, being Q_{gs}=+5.6 MeV. The importance of states with different spin and parity has been also evidenced.

As a further step we found it interesting to investigate another system whose ground to ground state Q-value is close to zero for neutron transfers, matching their optimum Q-value ($\sim$ 0 MeV). The ^{60}Ni+^{116}Sn system is very suitable in this sense, since it has Q_{gs}^{+1n}= − 1.7 MeV and Q_{gs}^{+2n}= + 1.3 MeV. One then expects to have a main population close to the ground to ground state transitions and, in particular for the +2n channel, it is interesting to see how calculations including only transfer to the 0^+_{gs} states compare with the experimental data. We present below some preliminary results of the sub-barrier transfer reaction ^{116}Sn+^{60}Ni performed using the magnetic spectrometer PRISMA [14, 15].

2. The experiment and experimental results

The experimental conditions for the measurement of the ^{116}Sn+^{60}Ni system were similar to those already successfully exploited in the ^{96}Zr+^{40}Ca case [11, 16]. By employing inverse kinematics and by detecting ions at very forward angles, we have, at the same time, enough kinetic energy of the outgoing recoils (for energy and therefore mass resolution) and a forward focused angular distribution thet results in a high detection efficiency. We measured an excitation function with a ^{116}Sn beam delivered by the heavy ion PIAVE injector and the ALPI superconducting booster of the Laboratori Nazionali di Legnaro with an average current of $\sim$ 2 pnA onto a 100 μg/cm^2 ^{60}Ni target with a C-backing of 15 μg/cm^2. Ni-like recoils have been detected by PRISMA at θ_{lab}=20°, corresponding to $\theta_{c.m.} \simeq 140°$. The bombarding energy of ALPI was varied in steps of

$\simeq$ 10 MeV from 500 to 410 MeV. In order to optimize the time loss due to the energy changes with ALPI some points have been measured by placing in front of the Ni targets one C-foil with a thickness of $\sim$ 85 μg/cm^2, in such a way to degrade the ^{116}Sn beam by about 7 MeV. Two energies, E$_{lab}$= 220 and 280 MeV, have been used with the Tandem only, to have a precise energy reference.

A complete excitation function has been measured from the Coulomb barrier to $\simeq$ 25% below, measuring the transfer yields down to $\sim$ 16 fm of distance of closest approach. Two monitor detectors were used for the relative normalization of different runs and for absolute cross section determination, by measuring the Rutherford scattered Ni and C ions. The two monitors allowed also to control the beam conditions on the target.

The identification of the reaction products in PRISMA is based upon the reconstruction of the trajectories of the ions, on an event-by-event basis [15, 17]. The trajectories are reconstructed through the positional and timing information provided by the start [18] and focal plane [19] detectors of PRISMA and by applying the equation of motion of a charged particle in the quadrupole and dipole magnetic fields. To obtain a fast algorithm for the off-line sorting phase of the data, the trajectory is assumed to be planar. Under this assumption the trajectories are uniquely defined by only one parameter, the bending radius ρ in the dipole. The effects of the fringing fields are taken into account considering an effective length for the magnetic elements of the spectrometer. The assignment of the atomic number Z is obtained by using the energy loss ΔE and the total kinetic energy E of the ions as provided by the ionization chamber. The reconstruction of the mass number A, is based on the relation $A/q \propto B\rho/v$ which follows from the Lorentz equation, here v is the velocity of the ion, which is given by $v = L/TOF$, being L the length of the trajectory.

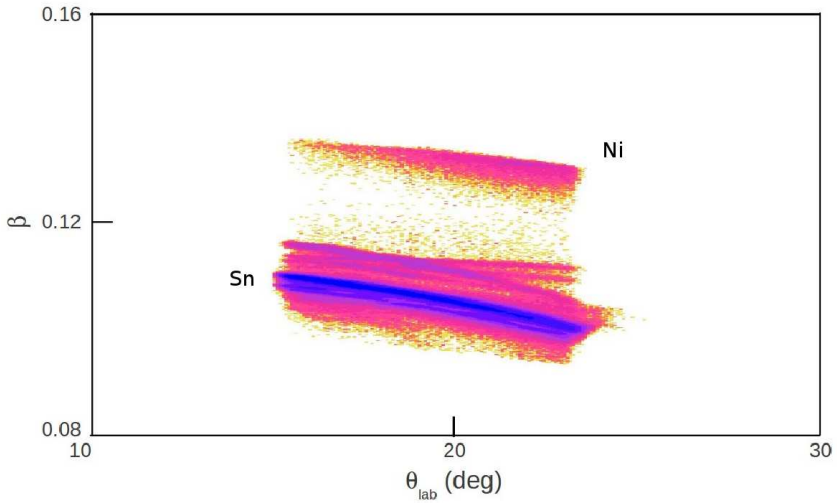

Figure 1. Matrix velocity ($\beta = v/c$) vs θ_{lab} scattering angle for the reaction ^{116}Sn+^{60}Ni at E$_{lab}$=500 MeV and PRISMA placed at θ_{lab}=20° (see text for details).

In Fig. 1 we show an example of matrix velocity ($\beta = v/c$) versus scattering angle θ_{lab} at the bombarding energy of E$_{lab}$=500 MeV. The magnetic fields have been set to detect Ni-like ions, but part of the Sn-like ions have magnetic rigidities which allow them to pass through the spectrometer and reach the focal plane detectors. From the matrix one sees how the two ions are well separated.

Due to the existence of several atomic charge states q, different A/q values are obtained for each Z and a selection of each single charge state is needed to construct the mass spectra.

From the Lorentz equation it is possible to derive the proportionality $E \propto q\rho\beta$, thus from a two-dimensional matrix $\rho\beta$ versus E one can select the atomic charge states, as shown in Fig. 2, where the separation among the different q is clear.

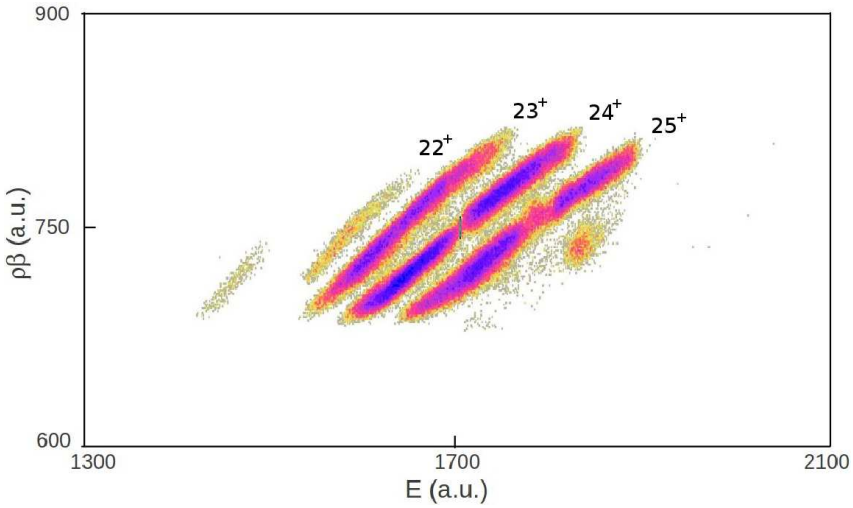

Figure 2. $\rho\beta$ versus E matrix, constructed to select the different atomic charge states of Ni-like ions. The central structure in the matrix corresponds to the most probable charge state q=24^+. The assignment of the other q values is given correspondingly.

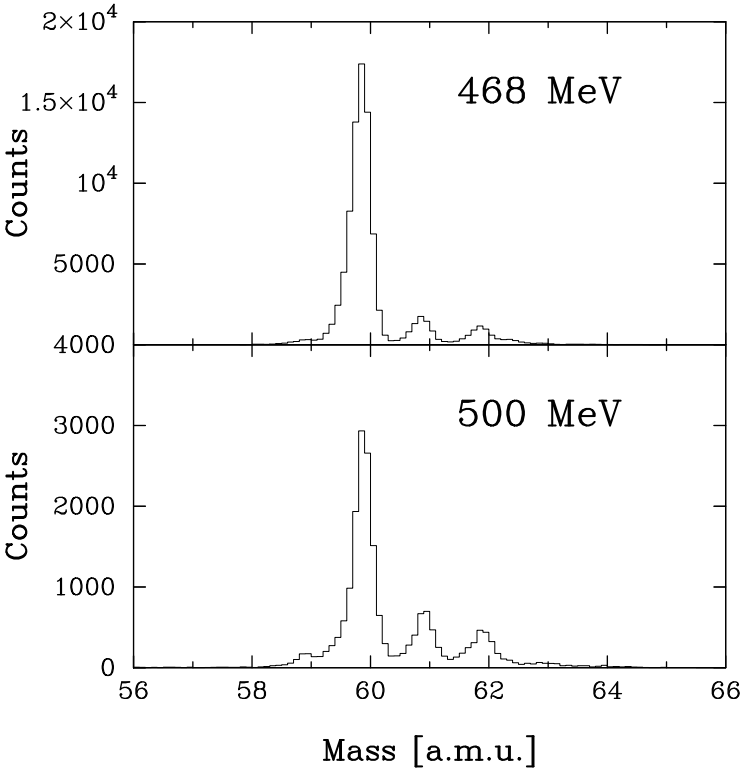

Figure 3. Mass spectra obtained at the indicated bombarding energies for the Ni-like ions.

All charge states are finally added together in order to obtain the mass spectra. Two mass spectra for Ni isotopes are displayed as examples in Fig. 3, showing the clear separation obtained for the different transfer channels. The two plots correspond to energies well above the Coulomb barrier (E_{lab}=500 MeV) and close to the barrier (E_{lab}=468 MeV). While in this last case only neutron pick-up channels are present, as expected from simple optimum Q-value arguments, at the higher energy one sees the onset of neutron stripping channels, which are derived for the presence of complex mechanisms involving large energy losses and consequent neutron evaporation from the primary fragments [1, 20, 21, 22].

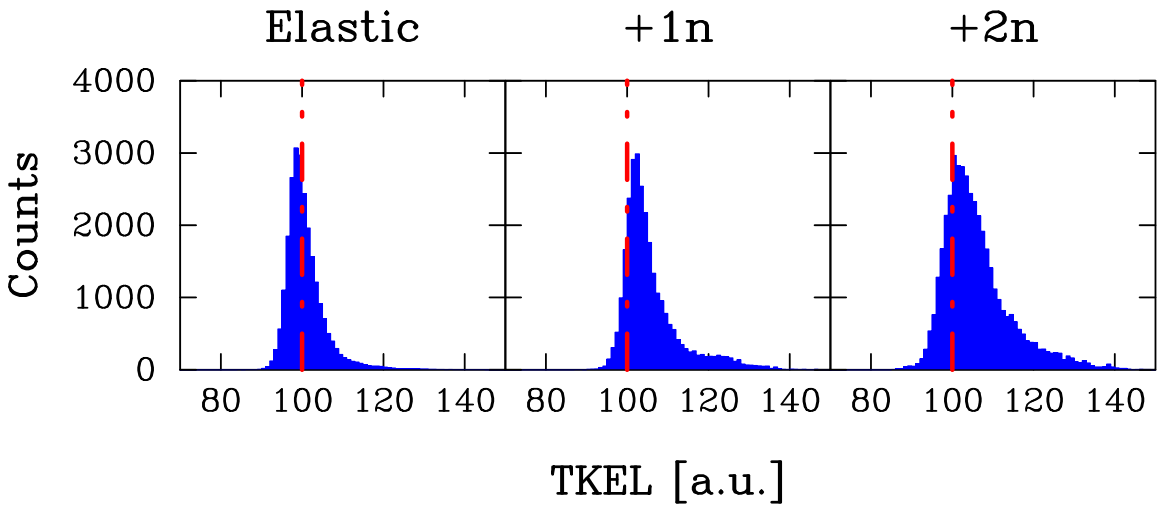

Figure 4. TKEL loss spectra for the elastic and +1n, +2n transfer channels at the bombarding energy E_{lab} = 475 MeV. See text for details.

In Fig. 4 we display the Total Kinetic Energy Loss (TKEL) spectra for the elastic and one ($+1n$) and two ($+2n$) neutron pick-up channels at the representative bombarding energy of E_{lab} = 475 MeV, close to the Coulomb barrier. The elastic(+inelastic) peak has a width of $\sim$ 3 MeV, close to the expected energy resolution. With vertical dashed lines are indicated the position of the Q-value for the elastic scattering. The elastic channel (Q_{gs}=0) is taken as reference (channel 100 in the figure). For neutron transfers Q_{gs}^{+1n}= $-$ 1.7 MeV and Q_{gs}^{+2n}= + 1.3 MeV and one observes a significant population close to these (ground to ground state) Q-values. At the same time one sees a tail toward larger TKEL, more marked for the $+2n$ channel, typical of the energy regime close to the barrier. These energy loss components tend to disappear far below the barrier.

At present stage the data are being analyzed in the whole measured energy range, with the main aim to extract the transfer cross sections for the one and two neutron pick-up channels and for channels involving proton stripping. Proton stripping channels are in general more difficult to get experimentally far below the barrier since they drop off more rapidly than neutron channels, therefore a careful evaluation of the angular distribution (and transmission of the spectrometer) is mandatory. The $-1p$ channel, together with the $+1n$ channel, is one of basic building blocks defining the more complex multiple particle transfer and the comparison of its behaviour as function of the bombarding energy with the microscopic calculations will tell about the shape of the form factors [23].

3. Evaluation of the PRISMA response function

In the present experiment part of the excitation function for transfer channels has been performed with sufficient statistics to allow making cuts in the angular acceptance of PRISMA. In this way differential cross sections may be extracted for different angles at each energy, thus increasing significantly the number of points which define the transfer probability as a function of the distance of closest approach. Thus, a careful evaluation of the PRISMA response function has to be studied to assess the influence of the transport of the ions through the spectrometer on the measured yields. A successful application of these studies has been employed in the case of the ^{48}Ca+^{64}Ni system [17, 24] where experimental angular distributions for elastic as well as for transfer channels, have been corrected for the response of the spectrometer. Such corrections involved a case where measurements have been performed at energies much higher than the Coulomb barrier and where deep-inelastic components contribute significantly to the yields. In the case of sub-barrier energies the Q-value distributions are quite narrow, as has been shown in Fig. 4, and one expects that the effect of the transmission is relevant mostly at the very edge of the spectrometer.

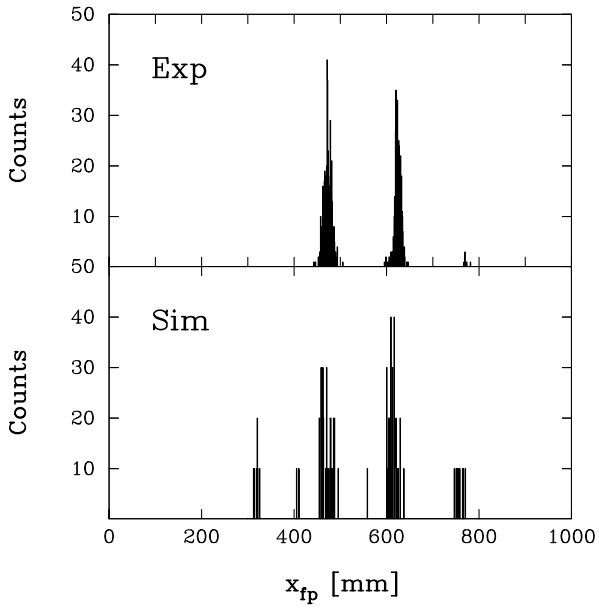

Figure 5. Focal plane distribution (in-plane position coordinate x_{fp}) of the charge states for the central trajectories of the elastic channel (^{60}Ni) at E_{lab} = 440 MeV. In the top panel are the experimental data, in the bottom panel the simulated events. The agreement between the two distributions reflects the correct settings of the magnetic fields in the simulation.

The response function of the spectrometer has been extracted via a MonteCarlo simulation, taking into account the kinematics of the reaction and the geometry of the magnetic elements and detectors [17]. The calculations have been done at the bombarding energy of E_{lab} = 440 MeV, which corresponds to a value below the Coulomb barrier and in the middle of the excitation function where the experimental yield is very large. Calculations have been applied as a first step to the elastic channel, which almost coincides with the Rutherford scattering, thus allowing to properly test the validity of the procedure.

To calculate the response function we give as input to the simulation code a known initial distribution of scattered events, in this case isotropic and uniform within a given energy range.

The code then creates a data-file with all the parameters detected with PRISMA. This file is then sorted with the same code used to analyze the experimental data. The response function f is then defined, as a function of the scattering angle θ_{lab} and the kinetic energy of the detected ions E, by the ratio $f(\theta_{lab}, E) = N_o(\theta_{lab}, E)/N_i(\theta_{lab}, E)$ where N_o and N_i are the number of events detected at the end of the transport and given as input to the code, respectively. This ratio is then used to correct for the original experimental yields. The procedure employs a ray tracing code which uses numerical integrators to determine the trajectories of individual rays through the electromagnetic fields. The calculation starts by generating a distribution that is uniform in energy and isotropic in angle, covering the energy range between 320 and 400 MeV and the angular range $\theta_{lab} = 12° - 28°$ and $\phi_{lab} = \pm 32°$. This distribution is then transported to the focal plane by the ray tracing code outlined above, using the magnetic field settings of the experiment (i.e. $B_{max} = 0.7506$ T and 0.5690 T for the dipole and quadrupole magnet, respectively). The angular range is slightly larger than the acceptance of PRISMA which is defined by the entrance area of the quadrupole, while the energy range corresponds to the momentum acceptance of the spectrometer for ^{60}Ni ions, wider than the one covered by the reaction.

In Fig. 5 we show the experimental and simulated atomic charge state distribution for the elastic channel for the chosen energy. One sees the quite good agreement of the focal plane position between the simulated and experimental data. We remind that that at this stage the comparison with the experiment has to be intended as qualitative since the calculated charge state distribution is obtained by using a uniform distribution in energy and angle.

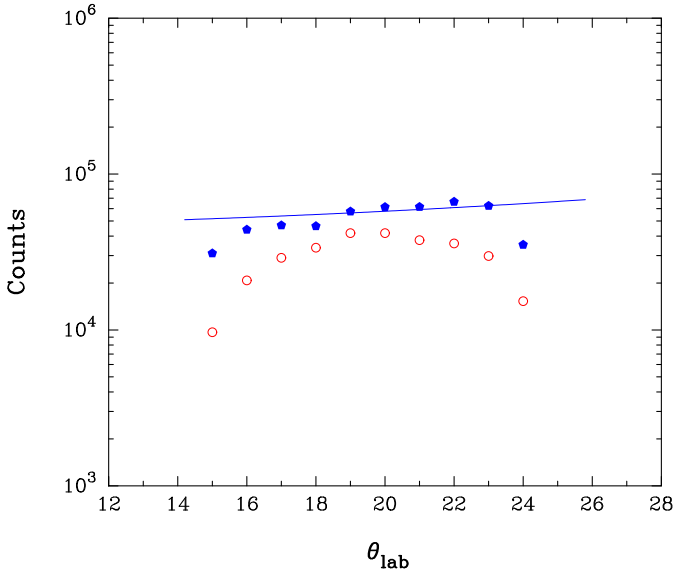

Figure 6. Angular distribution for the elastic channel (^{60}Ni) at E_{lab} = 440 MeV before (red symbols) and after (blue symbols) the correction for the response function. The solid line is the angular distribution for Rutherford scattering, normalized to the experimental data.

The results of the application of the response function on the experimental yields are shown in Fig. 6. Here, with a solid line we plot the angular distribution for the Rutherford scattering, with red dots the experimental data before the correction and with blue symbols the data after correction. One sees that the reconstructed experimental distribution follows quite well the Rutherford scattering in almost the whole angular range, with the exception of the extreme edges. The corresponding events belong in fact to the borders of the start detector, where the

presence of trajectories not entering into the spectrometer is much more probable than in the rest of the solid angle covered by the detector. Similar calculations are now being performed for the neutron transfer channels and for all other measured energies.

4. Conclusions

We performed an experiment to measure an excitation function for the main transfer channels in the ^{116}Sn+^{60}Ni, from above to well below the Coulomb barrier. The experiment has been done in inverse kinematics, with the lighter target-like ions detected with the magnetic spectrometer PRISMA. Good nuclear charge amd mass resolutions has been achieved over the whole energy range. Part of the excitation function has been measured with sufficient statistics to extract angular distributions. For this reason, a study of the PRISMA response function need to be done. Data analysis is in progress to deduce the cross sections and transfer probabilities for neutron pick-up channels as well as for channels involving proton stripping. The comparison between data and theory for the present case and for the previously measured ^{96}Zr+^{40}Ca system, namely superfluid and near closed shells nuclei, will significantly improve our understanding of nucleon-nucleon correlations in the transfer process.

5. Acknowledgments

The authors wish to thanl the LNL Tandem-ALPI stuff for providing us with the good quality beams and the target laboratory for the excellent target preparation. This work was partly supported by the European Community FP6 - Structuring the ERA - Integrated Infrastructure Initiative - contract EURONS No. RII3-CT-2004-506065. This work was, also, supported in part by the Croatian Ministry of Science, Education and Sports, Grant No. 0098-1191005-2890.

References

[1] L. Corradi, G. Pollarolo and S. Szilner, J. of Phys. G: Nucl. Part. Phys. **36**, 113101 (2009).
[2] B.F. Bayman and J.Chen, Phys. Rev. **C26**, 1509 (1982).
[3] R. Künkel, W. von Oertzen, H.G. Bohlen, B. Gebauer et al., Z. Phys. A **336**, 71 (1990).
[4] W. von Oertzen, I. Peter, S. Thummerer, H. G. Bohlen, B. Gebauer et al., Eur. Phys. J. A **20**, 153 (2004).
[5] A.H. Wuosmaa, K.E. Rehm, B.G. Glagola, Th. Happ, W. Kutschera, and F.L.H. Wolfs, Phys. Lett. B **255**, 316 (1991).
[6] K.E.Rehm, B.G.Glagola, W.Kutschera, F.L.H.Wolfs, H.Wuosmaa, Phys. Rev. C **47** , 2731 (1993).
[7] R. R. Betts, P. M. Evans, C. N. Pass, N. Poffe et al., Phys. Rev. Lett. **59**, 978 (1987).
[8] R. B. Roberts, S. B. Gazes, J. E. Mason, M. Satteson et al., Phys. Rev. C **47**, R1831 (1993).
[9] C. L. Jiang, K. E. Rehm, Gehring J., Glagola B. et al, Phys. Lett.. B **337**, 59 (1994).
[10] C. L. Jiang, K. E. Rehm, H. Esbensen et al., Phys. Rev. C **57**, 2393 (1998).
[11] L. Corradi, S. Szilner, G. Pollarolo et al., Phys. Rev. C **84**, 034603 (2011).
[12] E.Maglione, G. Pollarolo, A. Vitturi, R. A. Broglia and A. Winther, Phys. Lett. **B162**, 59 (1985).
[13] J.H.Sorensen and A.Winther, Nucl. Phys. A **550**, 306 (1992).
[14] A.M. Stefanini et al., Nucl. Phys. A**701**, 217c (2002).
[15] S. Szilner, C. Ur, L. Corradi, G. Pollarolo et al., Phys. Rev. C **76**, 024604 (2007).
[16] L. Corradi, S. Szilner, G. Pollarolo et al., Eur. Phys. J. Conf. Series **17**, 08004 (2011).
[17] D. Montanari, E. Farnea, S. Leoni, G. Pollarolo et al., Eur. Phys. J. A **47**, 4 (2011).
[18] G. Montagnoli, A.M. Stefanini, M. Trotta et al, Nucl. Instrum. and Methods **547**, 455 (2005).
[19] S.Beghini, L. Corradi, E.Fioretto et al, Nucl. Instrum. and Methods **551**, 364 (2005).
[20] L. Corradi, A. M. Vinodkumar, A. M. Stefanini, E.Fioretto et al., Phys. Rev. C **66**, 024606 (2002).
[21] S. Szilner, L. Corradi, G. Pollarolo, S. Beghini et al., Phys. Rev. C **71**, 044610 (2005).
[22] S. Szilner, L. Corradi, F. Haas, D. Lebhertz et al., Phys. Rev. C **84**, 014325 (2011).
[23] J.M. Quesada, G. Pollarolo, R. A. Broglia, A. Winther, Nucl. Phys. A **442**, 381 (1985).
[24] D. Montanari, S. Leoni, L. Corradi, G. Pollarolo et al., Phys. Rev. C **84**, 054613 (2011).
[25] A. Lemasson, A. Navin, N. Keeley, M. Rejmund et al., Phys. Rev. C **82**, 044617 (2010).